applied sciences

Article

Randomly Distributed Passive Seismic Source Reconstruction Record Waveform Rectification Based on Deep Learning

Binghui Zhao, Liguo Han *, Pan Zhang , Qiang Feng and Liyun Ma

College of Geo-Exploration Science and Technology, Jilin University, Changchun 130026, China; zbh21@mails.jlu.edu.cn (B.Z.); zhangpan@jlu.edu.cn (P.Z.); fengqiang20@mails.jlu.edu.cn (Q.F.); maly22@mails.jlu.edu.cn (L.M.)
* Correspondence: hanliguo@jlu.edu.cn

Abstract: In passive seismic exploration, the number and location of underground sources are very random, and there may be few passive sources or an uneven spatial distribution. The random distribution of seismic sources can cause the virtual shot recordings to produce artifacts and coherent noise. These artifacts and coherent noise interfere with the valid information in the virtual shot record, making the virtual shot record a poorer presentation of subsurface information. In this paper, we utilize the powerful learning and data processing abilities of convolutional neural networks to process virtual shot recordings of sources in undesirable situations. We add an adaptive attention mechanism to the network so that it can automatically lock the positions that need special attention and processing in the virtual shot records. After testing, the trained network can eliminate coherent noise and artifacts and restore real reflected waves. Protecting valid signals means restoring valid signals with waveform anomalies to a reasonable shape.

Keywords: convolutional neural networks; improved Res-U-net; denoising; passive seismic; reconstruction

check for updates

Citation: Zhao, B.; Han, L.; Zhang, P.; Feng, Q.; Ma, L. Randomly Distributed Passive Seismic Source Reconstruction Record Waveform Rectification Based on Deep Learning. *Appl. Sci.* **2024**, *14*, 2206. https://doi.org/10.3390/app14052206

Academic Editor: Roberto Scarpa

Received: 25 January 2024
Revised: 2 March 2024
Accepted: 4 March 2024
Published: 6 March 2024

1. Introduction

In seismic surveys, noise in the subsurface tends to interfere with effective signals. Its signal is weak but widely distributed and haphazard, and we often resort to various techniques to eliminate it. However, waves generated by vibrations from underground sources will carry information about underground tectonics as they propagate. If noise can be used, it can act as a substitute for an active source. In some cases where active source excitation is not possible, such as near cities, it is sufficient to set up geophones to receive passive sources of signals. At the same time, passive acquisition is cost-effective because there is no need to excite seismic sources. Furthermore, due to the rich frequency range of subsurface noise sources, there are a large number of low-frequency signals [1]. Therefore, passive sources are more advantageous than active sources in large-scale, deep seismic surveys.

After acquiring the passive source seismic record, we can use seismic interferometry [2,3] to reconstruct the passive source seismic record into a virtual shot record similar to the active source seismic shot record. However, using seismic interferometry to reconstruct passive seismic data inevitably results in coherent noise and artifacts. The noise has a greater impact on deteriorating the reconstruction of seismic data when the attenuation of the medium is high [4]. Removing the effects of this coherent noise and artifact disturbances is an ongoing effort by geophysicists. The F-K [5] filtering-based processing can suppress the coherent noise to some extent, but it may cause damage to the effective wave. Suppressing the coherent noise in the Radon domain has also been tried several times [6–8], but there is still a problem of low resolution. Rabiner et al. [9] created a median filtering denoising method and later produced many derivative algorithms [10,11]. They can operate on pixels on the image, but their small windows have no effect on coherent noise and artifacts, and large windows will blur effective signals.

The above methods can remove coherent noise and artifacts to some extent. However, they can harm the effective signal or suppress it poorly. The selection of parameters will have a large impact on the processing effect, which is somewhat subjective. In addition, this method cannot effectively recover the effective waveform.

Deep learning learns deep features of images and other information by training neural networks. LeCun [12] and others first invented a convolutional neural network and achieved good results in handwritten digit recognition. The AlexNet, invented by Hinton et al. [13], has achieved good results in image recognition and won the championship in the image recognition contest, setting off an upsurge of in-depth learning. Since then, various deep learning networks have sprung up in the public's view, such as VggNet [14], ResNet [15], FCN [16], DnCNN [17], and UNet [18]. These networks have achieved good results in classification and image segmentation. Based on ensuring the accuracy of manual recognition and conventional methods, they have higher processing efficiency, so they have been widely developed in various fields.

In recent years, thanks to the upgrading of computer hardware resources, deep learning algorithms have been widely used in the geophysical field. Gu et al. [19] realized low-frequency reconstruction in full-waveform inversion based on deep learning. Parasyris et al. [20] synthetic data generation for deep learning-based inversion for velocity model building. Zhang et al. [21] used interactive salt segmentation from 3D seismic images using saltisnet3d. Tao et al. [22] acoustic impedance inversion of seismic imaging profiles using self-attentive U-Net. Xiong et al. [23] use SafeNet to identify seismic disturbances. Sun et al. [24] accomplished low-frequency extrapolation of multicomponent data in Elastic FWI using deep learning. Wang et al. [25] used the MCMC inverse problem method of neural networks to perform numerical simulations in GPR cross-hole full waveform inversion. Liu et al. [26] used fine-tuned FPN to achieve microseismic first-arrival pickup. Lou et al. [27] proposed MCDL to achieve seismic volume dip estimation. Dou et al. [28] used the "MDA GAN" of the adversarial network to realize 3D seismic data interpolation and reconstruction.

In this research, a convolutional neural network is used to identify and suppress the coherent noise and artifacts of the virtual shot record. We obtain passive seismic records with a small number of sources and passive seismic records with a large number of sources through forward simulation. Using seismic interferometry, they are reconstructed as virtual shot records, respectively. The reconstructed records of passive seismic records with fewer sources are used as training data, and the reconstructed records of passive seismic records with more sources are used as training labels. The network is utilized to mine the features of passive data with better passive seismic source effects. Using neural networks to suppress coherent noise and artifacts and restore waveforms in parts where waveforms are not continuous enough. For the virtual shot records with an uneven source distribution, we use the virtual shot records with a wide source distribution as labels. At this time, the task of the network is not only to suppress coherent noise and artifacts and restore the ductility and continuity of the waveform, but also to restore the event of linear intersection to the event of double curvature. Although they are two tasks, we use the same network model to implement them and take a large number of evenly distributed virtual shot records as the training labels for the two tasks. Therefore, if the above two conditions are not ideal when we are collecting passive sources, we can reduce their impact on our seismic records and finally obtain better results, which improves the applicability of passive seismic exploration.

2. Theory and Method

2.1. Cross-Correlation Seismic Interferometry

Seismic interferometry generally includes the cross-correlation method [29], the deconvolution method [30], and the cross-coherence method [31]. Although the multi-dimensional deconvolution method and cross-coherence method can alleviate the impact of fewer sources and uneven source distribution on the virtual shot to a certain extent, they still cannot achieve good results for very extreme source distribution. Here, we used the cross-correlation method, which is the most efficient and stable method, to reconstruct the seismic virtual shot. The reconstruction method of cross-correlation can be expressed as:

$$R(x_B, x_A, t) + R(x_B, x_A, -t) = \delta(x_{H,B}, x_{H,A})\delta(t) - T(x_A, -t) * T(x_B, t)$$

where $R(x_B, x_A, t)$ stands for the seismic response excitation at x_A and received at x_B; $R(x_B, x_A, -t)$ represents its noncausal part; $\delta()$ represents the Dirac function; and $T(x_A, t)$ and $T(x_B, t)$ represent the transmitted wave responses at x_A and x_B, respectively.

When we use the equation for the mutual correlation reconstruction, we keep the x_A channel unchanged and each of the remaining channels as x_B, respectively. Then, we can obtain the reconstruction record with the x_A channel vertex as the excitation point and all channels as the reception points according to the original position of each channel. The reconstruction results here can be divided into two parts: the uncaused part and the causal part. It is a fundamental assumption of seismic interferometry [32] that requires no loss in the medium and a uniform distribution of the sources. Having satisfied these assumptions, we consider the causal part to be symmetrical with the noncausal part. By flipping and summing the causal and non-causal parts, we can obtain a virtual shot record with a higher signal-to-noise ratio. As a result, it is possible to flexibly construct the virtual shot record of a shot point at any detector position when reconstructing passive source seismic data with seismic interferometry without knowing the real source location.

However, when the number of sources is small under not widely distributed conditions, this will lead to spurious reflections and discontinuities in the waveform of the axes. If the source distribution is not uniform, when the virtual source is located on the side where the source distribution is lower, the reflected wave will be anomalous to a straight line. In contrast, the false-shot recordings where the false seismic source is located on the side with more source distribution will have discontinuous reflected waves and artifacts.

2.2. Deep Learning Algorithms

Based on the above problems in the reconstruction process of non-extensive passive source distributions, we hope to restore virtual source records that conform to physical rules, have good continuity, weak coherent noise, and do not contain spurious axes. Here, we propose to use the UNet network for imperfect virtual shot records. Since the direct wave energy in the virtual shot records is strong and the reflected wave energy is weak, we introduced attentional gating (AG) [33] to add multiple attentional layers to the UNet, allowing it to focus more of its learning on the reconstruction of the reflected waves in the lower part of the record.

The AG, first proposed in the medical field, aims to mimic the human attention mechanism by targeting and focusing on salient features in the data, which can make the model more efficient. It enables local regions to receive special attention, automatically learning to focus on the structural features of the target, suppressing irrelevant regions of the input image, and highlighting features useful for a specific task. Validated on a dataset in the medical domain, the results obtained show that not only can it be integrated into a network model with minimal computational overhead, but it will also improve the flexibility and predictive performance of the network. Here, we adopt a lightweight CBAM attention mechanism [34] to make the network more capable of learning. When the network transforms a graph into a feature map, it can simultaneously generate specific feature map information on the channel and spatially. It also performs adaptive operations with the incoming feature maps and finally outputs the feature maps after the action of the attention mechanism. We drew inspiration from residual thinking in ResNet and added residual connections to the network to achieve optimal performance and reduce training difficulty. The network we used is shown in Figure 1.

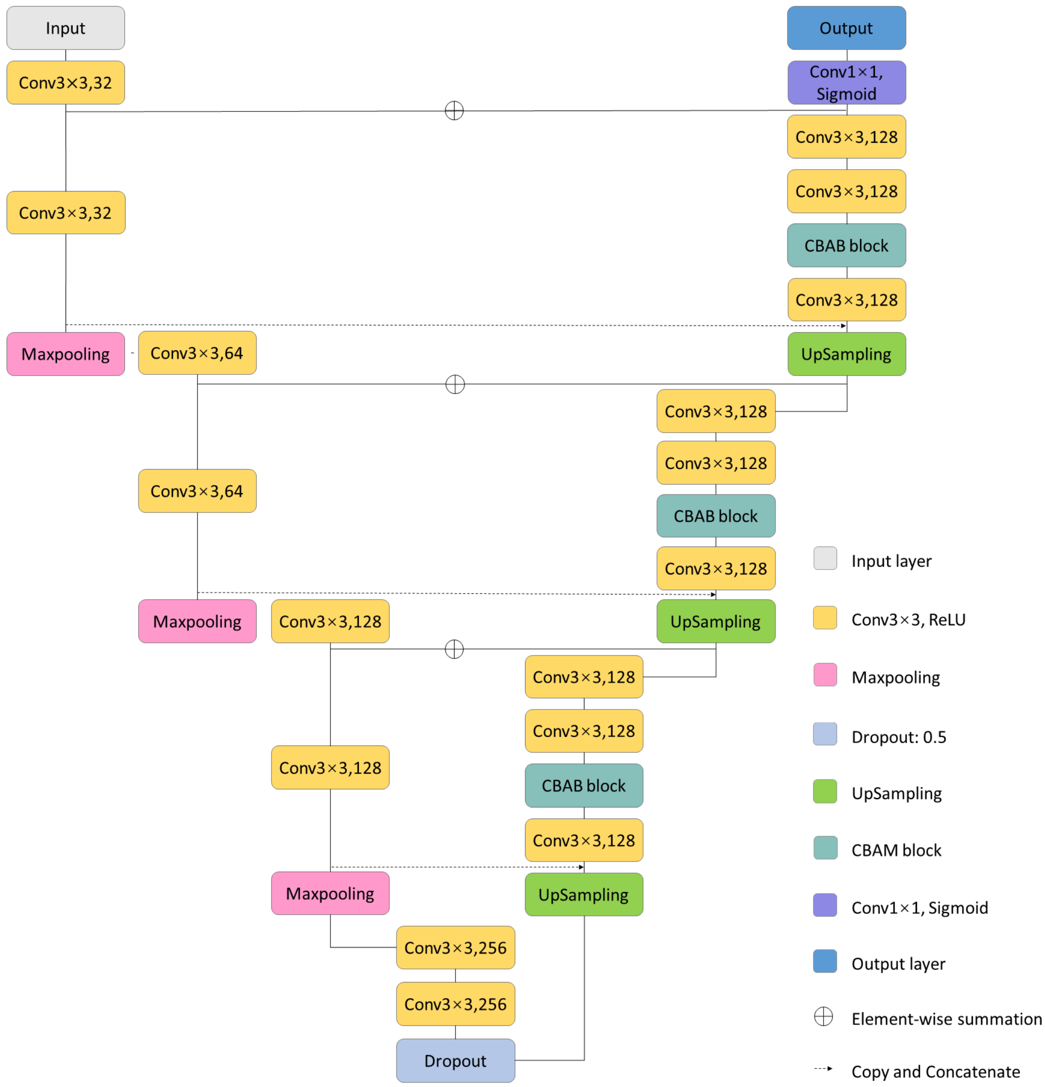

Figure 1. Network structure of improved U-net.

We used virtual shot records with fewer sources and unevenly distributed sources as training datasets, respectively. We used virtual shot records with more sources and randomly distributed in the subsurface as labels. We normalized the virtual shot records with the following equation:

$$x = \frac{x - x_{min}}{x_{max} - x_{min}}$$

where x represents the value of a point in the virtual shot record; x_{min} represents the minimum value in that record; and x_{max} represents the maximum value in that record. Here, we did not normalize the data using the extreme values in the whole data. This is to prevent anomalies in signal strength for some records. We also did not normalize the data using the usual per-track extremes. This is to prevent a blind-like imbalance in the processed data due to differences between seismic traces. We use single record normalization, using the maxima and minima of each virtual shot record to normalize, ensuring high contrast and continuity of pixel points horizontally for each record.

After preprocessing the data, we can then feed the processed dataset into our network. The optimizer is Adam; the activation function is ReLU except for the last layer, which is sigmoid; and the loss function is MSE:

$$loss(y_1, y_2) = \frac{1}{N} \sum_{i=1}^{N} (y_2 - y_1)^2$$

where N represents the sum of the number of pixels in a single seismic record; i represents the number of elements processed by the neural network; and y_2 and y_1 represent the predicted and target values (labels) of the network, respectively.

In general, there are some difficulties in using passive seismic reconstruction records as a dataset. If the active seismic record is chosen as the label, the valuable low frequency information in the passive source data will be lost. If the more effective virtual shot records are chosen as labels, some noise will inevitably be generated. In this paper, we believe that it is more important to protect the low-frequency signal. Therefore, for better, effect virtual shot records are chosen as labels.

3. Numerical Example

3.1. Enhanced Reconstruction Results for a Small Number of Seismic Sources

In this paper, virtual shot records are obtained from twenty velocity models. The velocity model as shown in Figure 2 will be used to obtain passive seismic records, which will be reconstructed into virtual shot records to be used as test data. These velocity models used to generate the training and test sets are randomly generated. To demonstrate the generalizability of the method, the test set is not included in the training set. Here the grid size of the velocity model is 2 m, the geophone spacing is 1 grid spacing, and the sampling interval is set to 1 ms to receive a total of 200 passive seismic records. Random noise sequences were used for the seismic sources. Each velocity model contains 128 seismic traces, and since the intercorrelation method allows the construction of shot points at any geophone point, 128 virtual shot point seismic records can be generated. To address the poor results of reconstructed records due to the small number of sources, we used them as training data and used reconstructed records with a large number of evenly distributed sources as labels. To compress the training cost and reduce unnecessary training, we only show the virtual shot records of the first 800 sampling points after reconstruction. We show the two source distributions as training sets and training labels under the velocity model (see Figure 3). The virtual shot records used as training data are obtained by reconstructing the passive source seismic records under the source distribution shown in Figure 3a. Under the distribution of seismic sources shown in Figure 3b, we reconstructed the virtual shot records as training labels. By inputting training data and training labels into the network, we can obtain a trained network. This network can process the waveforms of the virtual shot records.

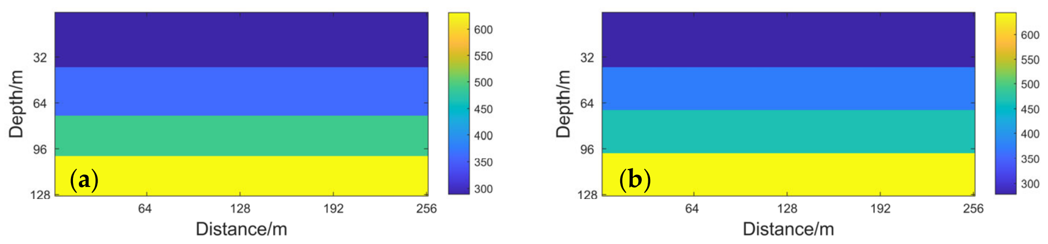

Figure 2. Velocity models used for the test data. (**a**) Test model 1; (**b**) test model 2.

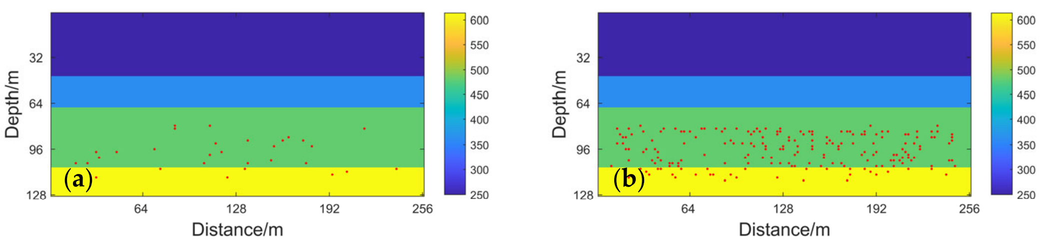

Figure 3. Completely randomized distribution of passive seismic sources. The red dots represent where the sources are located. (**a**) Distribution of a small number of sources. (**b**) Distribution of a large number of sources.

Our computing device was a Nvidia Quadro RTX 4000, and our neural network framework was TensorFlow-GPU 2.6.0 with 8 GB of video memory. To improve the generalization of the network, we set the batch size to 4, the learning rate to 0.00001, and gave a large dropout value of 0.5. We selected 2560 seismic records as training data and 256 seismic records as test data. After 1000 iterations, the loss of the network converges, and training is complete. The loss and decline of the network are shown in Figure 4. We fed the test data into the network, and the results are shown in Figures 5 and 6.

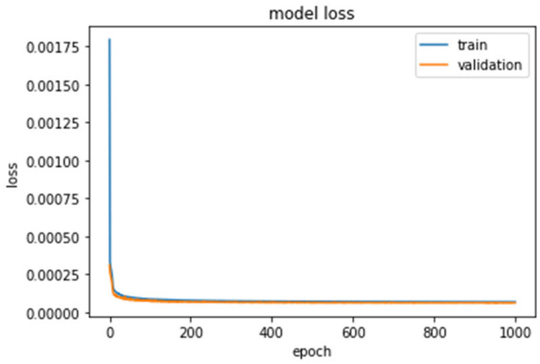

Figure 4. The loss convergence of the network.

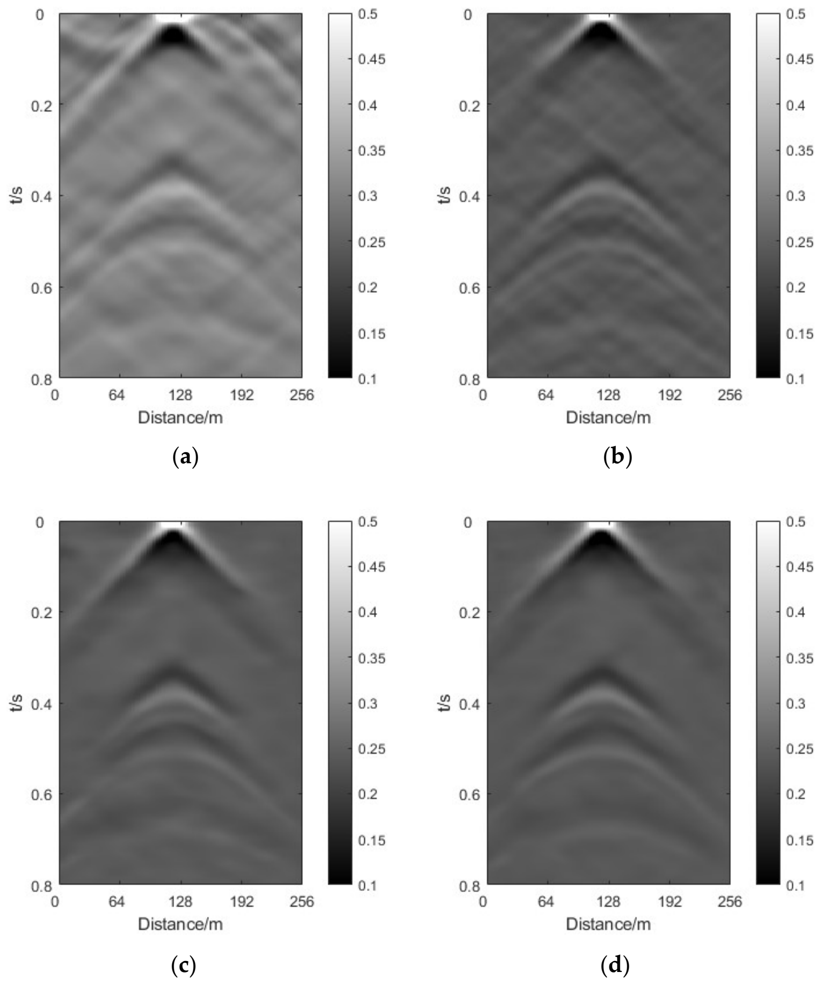

Figure 5. The processing results display virtual shot records with a small number of seismic sources under test model1. (**a**) A virtual shot of a small number of sources and input data. (**b**) A virtual shot of a large number of sources, labeled. (**c**) Processing result of attention mechanism UNet, prediction. (**d**) Processing result of improved network prediction.

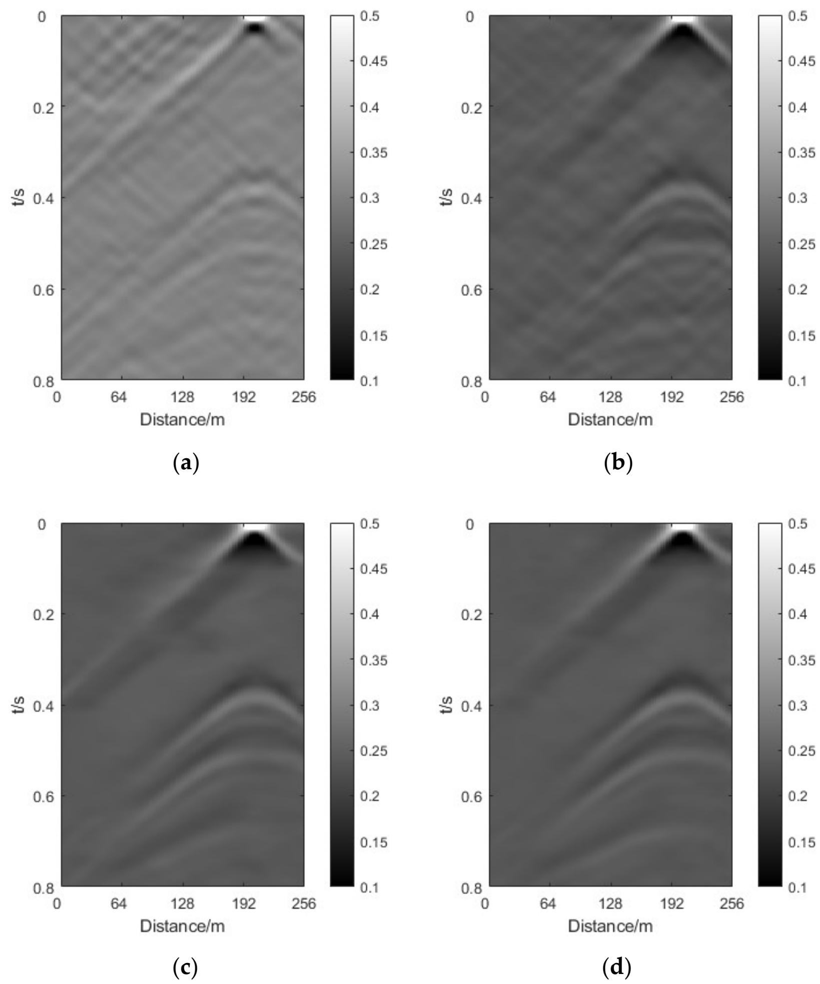

Figure 6. The processing results display virtual shot records with a small number of seismic sources under test model2. (**a**) A virtual shot of a small number of sources and input data. (**b**) A virtual shot of a large number of sources, labeled. (**c**) Processing result of attention mechanism UNet, prediction. (**d**) Processing result of improved network prediction.

To test whether the performance of our designed network is enhanced compared to the original network, we set the UNet neural network with attention mechanisms as the control group to test the improvement effect. By comparison, we can see that the coherent noise is effectively suppressed by the processing of the neural network. To solve the above problem that passive virtual shot records as labels may still be noisy, we found that both the training set and its labels contain a certain amount of coherent noise during the training process. However, due to the differences in objective factors such as their source locations and numbers, the training data and labels corresponding to the same virtual shot recordings under the same velocity model are similar in terms of effective waveforms when reconstructed, whereas the coherent noise in the virtual shot recordings is unmatchable. This also leads to the fact that our neural network does not learn the invalid features of the relevant noise during training. Although the labels also inevitably contain some coherent noise, which is an interesting finding in our suppression of coherent noise. Similarly, it is difficult for the neural network to learn the features of the artifacts because the features recorded by the virtual shot vary in each training data, and the corresponding virtual shot labels contain few or no artifacts in the same position. As a result, the artifacts are eliminated. In contrast, since the effective signals on the training data and corresponding labels are similar, our neural network can learn their features. Therefore, the weaker effective waveforms in the virtual shot records of a small number of sources are better protected and enhanced. In addition, where waveform discontinuities are present, our network complements them, restoring waveforms with good continuity.

Although these networks can suppress coherent noise and artifacts effectively, they also extract effective signals. However, it can be clearly seen that the improved network can suppress noise more thoroughly. The continuity of the same waveform axis is better and clearer, which also proves that our improvement of the network is effective.

In this section, we experiment with neural networks to reconstruct records of unevenly distributed seismic sources. Using the velocity model from the previous section, we can concentrate the subsurface seismic sources in a small region for numerical simulation. The resulting passive seismic source records are reconstructed into unevenly distributed virtual shot records. The distribution of seismic sources is shown in Figure 7.

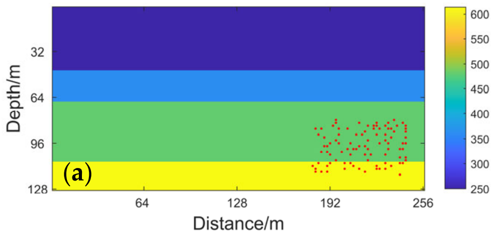

Figure 7. Schematic diagram of source distribution. The red dots represent where the sources are located. (**a**) Schematic diagram of inhomogeneous source distribution. (**b**) Schematic diagram of homogeneous source distribution.

After 400 iterations, our network was trained, and we fed the test data into the network, which was processed as shown in the figure. To test the generalizability of our network under different models and the processing performance for virtual shots located at different positions, we selected records of virtual shots located in multiple locations for display (see Figures 8 and 9).

Similar to the previous section, we can still use both of our neural networks to suppress coherent noise and artifacts. We can revert to a reasonable hyperbolic homogeneous axis in the virtual shot records on the side without the source distribution; we suppress the spurious homogeneous axis on the side with the source distribution. At the same time, the problem of insufficient continuation of the waveform is well resolved. We analyze that since there are many linear intersecting homography features in the training set corresponding to the hyperbolic homography axes in the training labels, it is possible to learn the corresponding features. The reason that coherent noise with artifacts can be suppressed is also similar to the previous section. In the tracts with the right side of the seismic distribution, our neural network recovers its waveform even though the training data are broken waveforms.

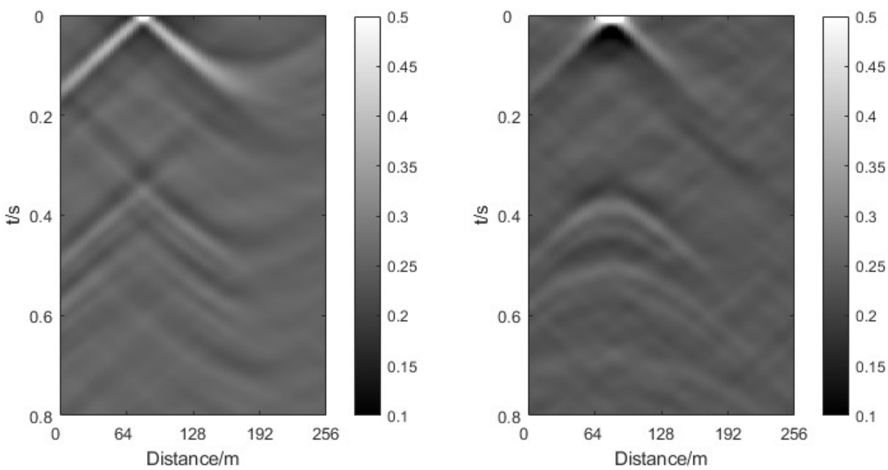

(**a**) (**b**)

Figure 8. *Cont.*

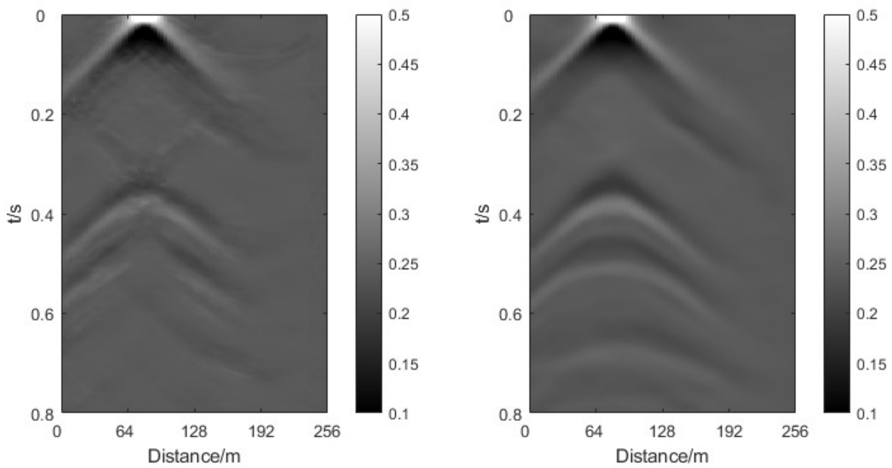

(**c**) (**d**)

Figure 8. The processing results display virtual shot records with uneven seismic sources under test model1. (**a**) A virtual shot of uneven seismic sources and input data. (**b**) A virtual shot of uniformly distributed sources, labeled. (**c**) Processing result of attention mechanism UNet prediction. (**d**) Processing result of improved network prediction.

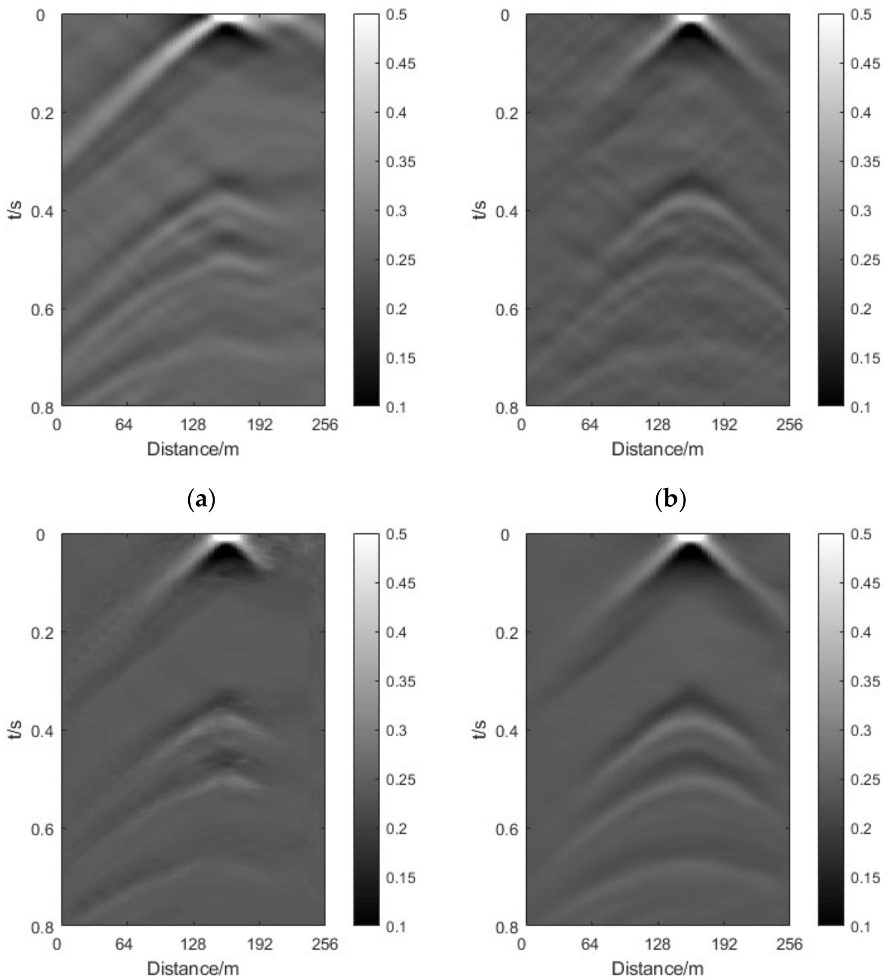

(**a**) (**b**)

(**c**) (**d**)

Figure 9. The processing results display virtual shot records with uneven seismic sources under test model2. (**a**) A virtual shot of uneven seismic sources and input data. (**b**) A virtual shot of uniformly

distributed sources, labeled. (**c**) Processing result of attention mechanism UNet prediction. (**d**) Processing result of improved network prediction.

In the testing of uneven source distribution, we can see that both networks can effectively suppress coherent noise and artifacts. However, when carefully comparing the processed waveforms, we found that the virtual records processed by the improved network showed clearer and more continuous waveforms.

3.2. Virtual Shot Record Processing under a Complex Model

In the experiment with the simple layered model, we have achieved good processing results for simple seismic records. When the velocity model becomes complex, the seismic record will inevitably become complex. In order to test the effect of our method on processing complex seismic records, we used the virtual shot record generated by the complex velocity models to train the neural network. The complex velocity models are shown in Figure 10, and their processing results are shown in Figures 11 and 12.

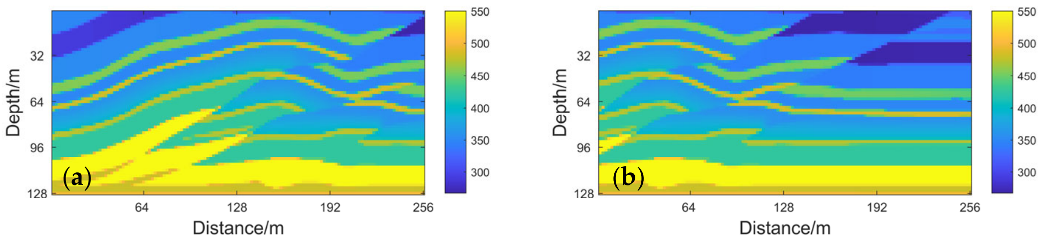

Figure 10. Complex velocity model of test data. (**a**) Test model 1; (**b**) test model 2.

Through the above comparison before and after processing, we can find that in the face of complex models, even if the number of sources is sufficient and the distribution is uniform, the virtual shot record is not perfect. In the face of imperfect processing tasks, the network processing effect is still good.

In the case of a small number of sources, our network can still remove a large number of virtual events and coherent noise from the virtual shot record and effectively restore the discontinuous events to continuous events.

In the case of dealing with unevenly distributed sources, the network also removes a large number of spurious events and coherent noise from the virtual shot recordings. It will also effectively reduce linear intersection events to hyperbolic events that conform to physical laws.

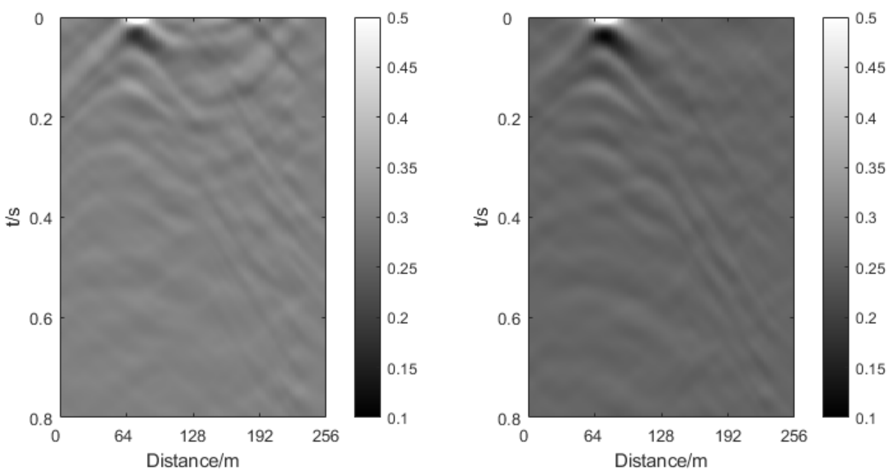

(**a**) (**b**)

Figure 11. *Cont.*

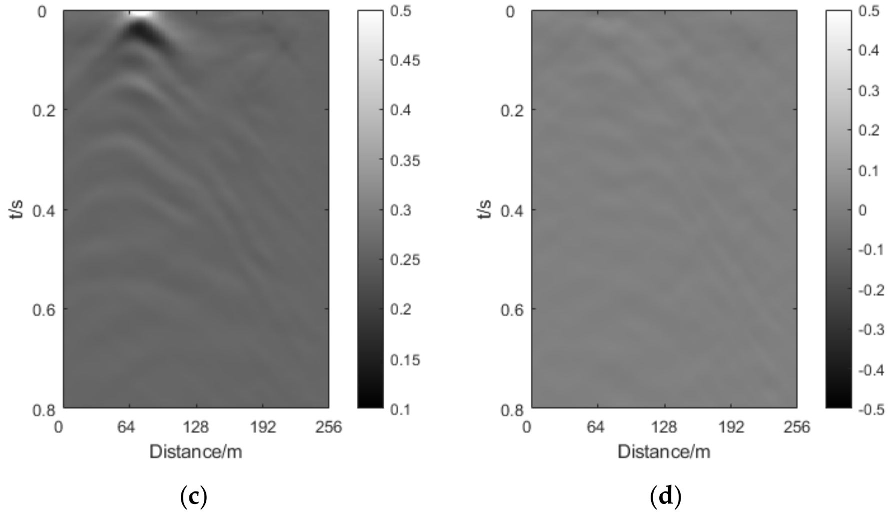

Figure 11. The processing results display virtual shot records with a small number of seismic sources under test model1. (**a**) A virtual shot of a small number of sources. (**b**) A virtual shot of a large number of sources, labeled. (**c**) Processing result of improved network prediction. (**d**) The residual between the processing result and the test label.

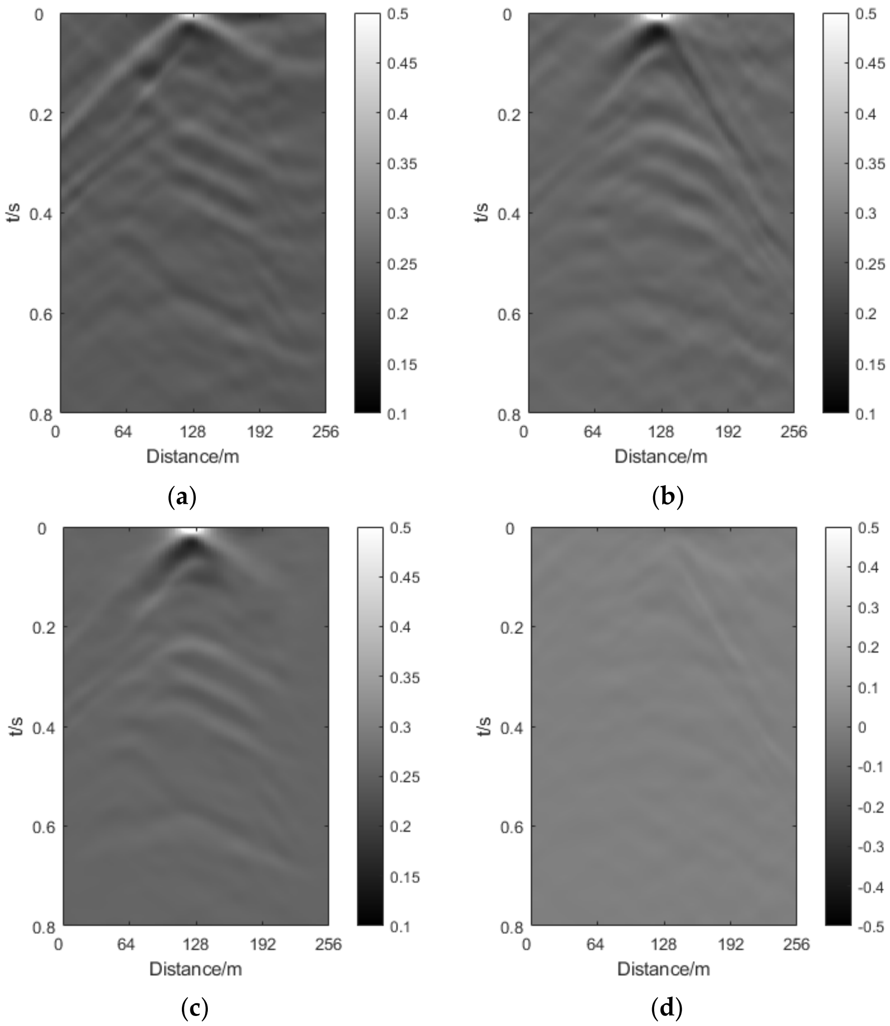

Figure 12. The processing results display virtual shot records with uneven seismic sources under test model2. (**a**) A virtual shot of uneven seismic distributed sources and input data. (**b**) A virtual shot of

uniformly distributed sources, labeled. (**c**) Processing result of improved network prediction. (**d**) The residual between the processing result and the test label.

It can be seen that our method has achieved good results not only in the simple layered model but also in the complex model. This result also proves that this method has wide applicability.

We can see that the waveforms in the wavefield become more complex in spite of the fact that the velocity model becomes complex, resulting in the waveforms in the wavefield becoming more complex. Our network still suppresses the coherent signal at a low level. For the virtual shot records of a small number of sources, the waveforms are clearer with our network processing. For the virtual shot records of sources distributed only on one side, the waveform anomalies are restored to a reasonable shape by our network processing.

After achieving good results in the processing of virtual shot records for conventionally small numbers of sources and for conventionally unevenly distributed sources, we tried to process the virtual shot records for extremely distributed sources. The two extremely distributed sources are shown in Figure 13. They are the sources located in the shallow space and the sources located in the narrow range, respectively.

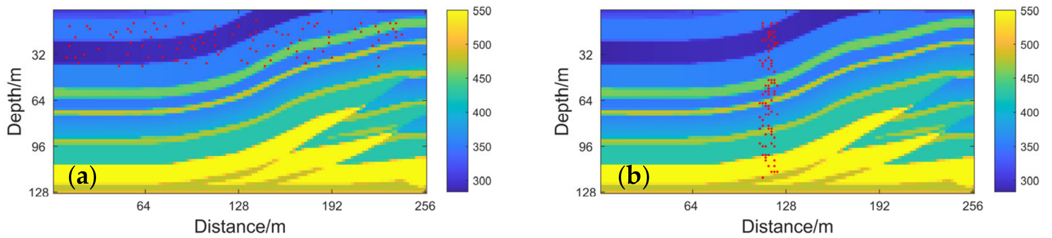

Figure 13. Schematic diagram of two extreme distributions of seismic sources. The red dots represent where the sources are located. (**a**) The sources are located in a shallow space. (**b**) The sources are located in a narrow range.

After processing using neural networks, the results are shown in Figures 14 and 15. It can be seen from the comparison figure that the virtual shot records corresponding to these two extreme signal source distributions contain a large number of spurious events and coherent noise. Moreover, the false reflections are stronger in the reconstructed records, and the ductility of the effective signal reflection waveform is not enough.

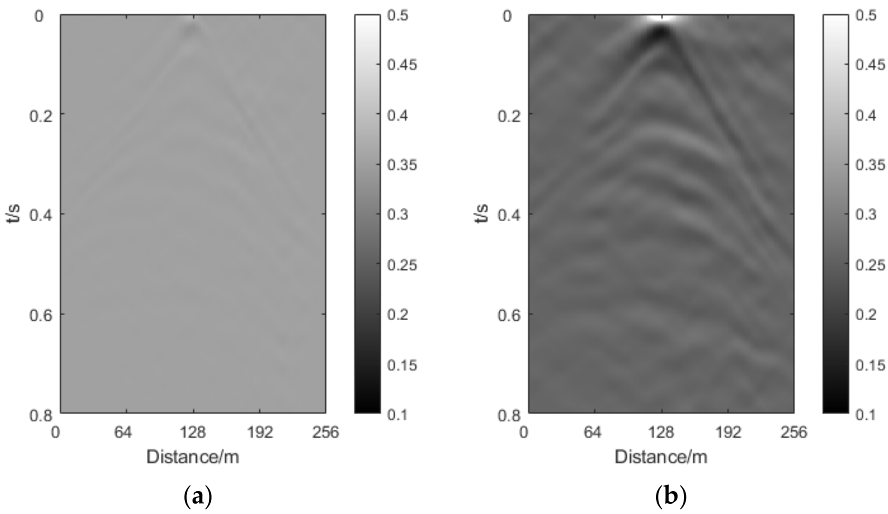

Figure 14. *Cont.*

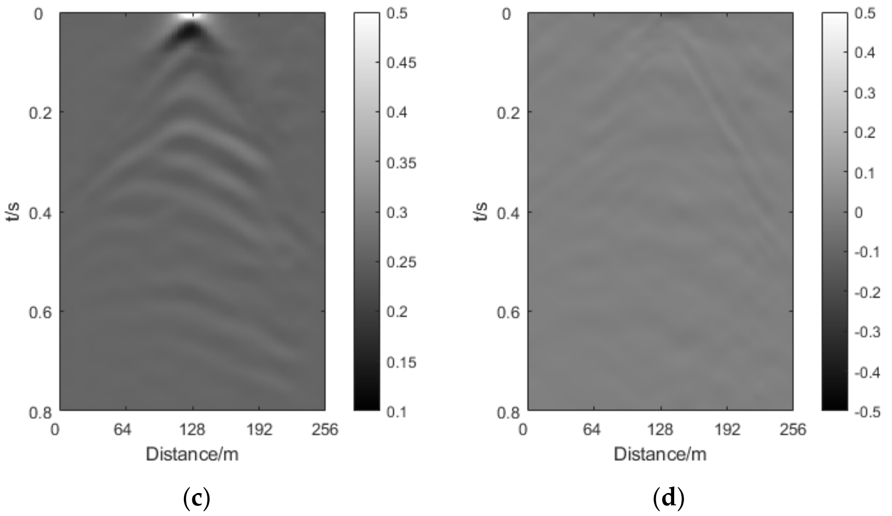

Figure 14. The processing results display virtual shot records with uneven seismic sources under test model1. (**a**) A virtual shot of shallow spaces distributed sources and input data. (**b**) A virtual shot of uniformly distributed sources, labeled. (**c**) Processing result of improved network prediction. (**d**) The residual between the processing result and the test label.

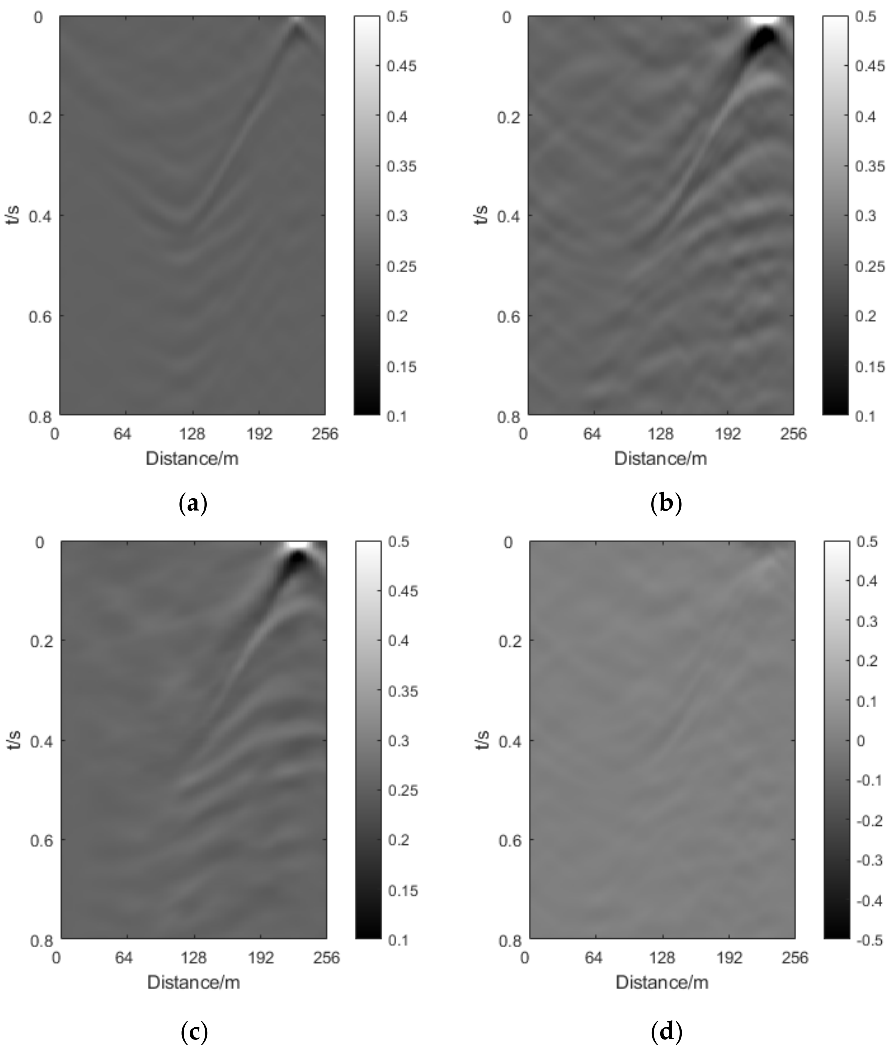

Figure 15. The processing results display virtual shot records with uneven seismic sources under test model1. (**a**) A virtual shot of narrow spaces distributed sources and input data. (**b**) A virtual shot of

uniformly distributed sources, labeled. (**c**) Processing result of improved network prediction. (**d**) The residual between the processing result and the test label.

After processing with the neural network, we successfully restored the waveform of the effective signal to a reasonable level. We can see from Figures 13 and 14 that the effective signal in the processed wavefield is stronger. It can be seen that our network can still recover effective signals from the artifacts and coherent noise.

4. Discussion

In passive-source seismic exploration, the number and distribution of subsurface sources are very random. The traditional seismic interferometry needs to satisfy the uniform distribution of the sources and be at a certain depth to reconstruct a high-quality virtual shot record. And the number and distribution location of undesirable seismic sources have a great impact on the virtual shot record.

Some conventional classical interferometric methods, such as inverse convolutional seismic interferometry [30], and algorithms developed on this basis, such as multidimensional deconvolutional seismic interferometry [35], can mitigate the effect of the inhomogeneous distribution of sources on the virtual seismic recordings to some extent. However, all of these methods require strict constraints on the uniform distribution of the geophones and the excision of the direct waves (which is very difficult to achieve for the noise sources). On this basis, the inverse is applied to the records received by all geophones. This operation is not only computationally huge, but the process is extremely unstable. These methods also do not give good results for specific source distributions (such as sources distributed in a narrow range on the survey line). In the method using deep learning, Sun et al. [36] used neural networks to make the virtual seismic record under uneven source distribution and learn the signal of the active source. Not only were a lot of artifacts eliminated, but the waveforms were also clearer. However, there is no discussion of the extreme case of distributed sources or the case of a small number of sources. And the use of active source records for labeling may cause some loss of low-frequency signals.

Compared with the improved seismic interferometry of the inverse convolution class, the cross-correlation-based seismic interferometry has fewer limitations, is computationally stable, and does not require strict uniform arrangement of geophones, cumbersome resection of direct waves, or computationally unstable inverse operations. And using the virtual seismic records of passive sources as labels for the training of the network can not only retain the low-frequency signals better but also train better due to the higher degree of similarity. Therefore, this method can improve the application effect of passive source seismic exploration to a certain extent on the basis of no additional requirements on the observation system and no loss of low-frequency signals. In this paper, we only show four of these cases of seismic source inactivity. After processing according to our network, the influence of the number and distribution of sources on the virtual seismic record can be reduced to some extent.

Only four of these inactive cases are shown in this paper. After the processing based on our network, the influence of the distribution of the seismic sources on the virtual shot records can be reduced to a certain extent. Therefore, this method can improve the application of passive source seismic exploration to some extent.

In the future development trend, with the future development of computing equipment and deep learning technology, there will be neural networks with better processing effects, which can solve the influence of the distribution of more complex seismic sources on the virtual shot record.

5. Conclusions

In this paper, a wavefield enhancement technique based on a convolutional neural network for passive seismic reconstruction records is proposed. The reconstructed virtual source records with a small number of sources and uneven source distribution are fed into the trained convolutional neural network, and the virtual source records with suppressed artifacts and coherent noise are obtained. The unphysical axes are restored to hyperbolic axes, and the low-frequency advantage of passive seismic surveys is retained.

Compared with reconstructed virtual shot recordings with a better number and distribution of sources, we retain accurate waveform information and low-frequency features with a lower proportion of noise. The network also has good generalization ability.

For passive sources that are not active in the subsurface, including the case where the number of sources is small and unevenly distributed, we provide a technical approach that ensures the effectiveness of passive seismic survey methods. It ensures high quality passive seismic reconstruction records when the sources are not widely distributed. The actual processing efficiency is high, and real-time monitoring can be realized.

Author Contributions: Methodology and manuscript writing, B.Z.; project administration and review, L.H.; experiments design guidance and review, P.Z.; investigation, Q.F.; validation, L.M. All authors have read and agreed to the published version of the manuscript.

Funding: This research was funded by the National Natural Science Foundation of China, grant numbers 42130805, 42074154, 42374147, and 42004106, the Natural Science Foundation of Jilin Province (no. YDZJ202101ZYTS020), and the Lift Project for Young Science and Technology Talents of Jilin Province (no. QT202116).

Data Availability Statement: The data presented in this study are available on request from the corresponding author.

Conflicts of Interest: The authors declare no conflicts of interest.

References

1. Bouchaala, F.; Vavryčuk, V.; Fischer, T. Accuracy of the master-event and double-difference locations: Synthetic tests and application to seismicity in West Bohemia, Czech Republic. *J. Seismol.* **2013**, *17*, 841–859. [CrossRef]
2. Draganov, D.; Wapenaar, K.; Thorbecke, J. Seismic interferometry: Reconstructing the earth's reflection response. *Geophysics* **2006**, *71*, SI61–SI70. [CrossRef]
3. Wapenaar, K.; Fokkema, J. Green's function representations for seismic interferometry. *Geophysics* **2006**, *71*, SI33–SI46. [CrossRef]
4. Bouchaala, F.; Ali, M.Y.; Matsushima, J.; Bouzidi, Y.; Takougang, E.T.; Mohamed, A.A.; Sultan, A.A. Scattering and intrinsic attenuation as a potential tool for studying of a fractured reservoir. *J. Pet. Sci. Eng.* **2019**, *174*, 533–543. [CrossRef]
5. Hale, D.; Claerbout, J.F. Butterworth dip filters. *Geophysics* **1983**, *48*, 1033–1038. [CrossRef]
6. Foster, D.J.; Mosher, C.C. Suppression of multiple reflections using the Radon transform. *Geophysics* **1992**, *57*, 386–395. [CrossRef]
7. Sacchi, M.D.; Porsani, M. Fast high resolution parabolic Radon transform. In Proceedings of the 1999 SEG Annual Meeting, Houston, TX, USA, 31 October–5 November 1999; OnePetro: Richardson, TX, USA, 1999.
8. Akerberg, P.; Hampson, G.; Rickett, J.; Martin, H.; Cole, J. Simultaneous source separation by sparse Radon transform. In Proceedings of the 2008 SEG Annual Meeting, Las Vegas, NV, USA, 9–14 November 2008; OnePetro: Richardson, TX, USA, 2008.
9. Rabiner, L.; Sambur, M.; Schmidt, C. Applications of a nonlinear smoothing algorithm to speech processing. *IEEE Trans. Acoust. Speech Signal Process.* **1975**, *23*, 552–557. [CrossRef]
10. Brownrigg, D.R.K. The Weighted Median Filter. *Commun. Assoc. Comput. Mach.* **1984**, *27*, 807. [CrossRef]
11. Liu, C.; Wang, D.; Liu, Y.; Wang, P.M.; Li, Q.X. Preliminary study of using 2D multi-level median filtering technique to eliminate random noises. *Oil Geophys. Prospect.* **2005**, *40*, 163–167.
12. LeCun, Y.; Boser, B.; Denker, J.S.; Henderson, D.; Howard, R.E.; Hubbard, W.; Jackel, L.D. Backpropagation applied to handwritten zip code recognition. *Neural Comput.* **1989**, *1*, 541–551. [CrossRef]
13. Krizhevsky, A.; Sutskever, I.; Hinton, G.E. Imagenet classification with deep convolutional neural networks. *Commun. ACM* **2017**, *60*, 84–90. [CrossRef]
14. Kataoka, H.; Iwata, K.; Satoh, Y. Feature evaluation of deep convolutional neural networks for object recognition and detection. *arXiv* **2015**, arXiv:1509.07627.
15. He, K.; Zhang, X.; Ren, S.; Sun, J. Deep residual learning for image recognition. In Proceedings of the IEEE Conference on Computer Vision and Pattern Recognition, Las Vegas, NV, USA, 27–30 June 2016; pp. 770–778.
16. Long, J.; Shelhamer, E.; Darrell, T. Fully convolutional networks for semantic segmentation. In Proceedings of the IEEE Conference on Computer Vision and Pattern Recognition, Boston, MA, USA, 7–12 June 2015; pp. 3431–3440.
17. Zhang, K.; Zuo, W.; Chen, Y.; Meng, D.; Zhang, L. Beyond a Gaussian Denoiser: Residual Learning of Deep CNN for Image Denoising. *arXiv* **2016**, arXiv:1608.03981. [CrossRef]
18. Ronneberger, O.; Fischer, P.; Brox, T. U-net: Convolutional networks for biomedical image segmentation. In *Medical Image Computing and Computer-Assisted Intervention–MICCAI 2015, Proceedings of the 18th International Conference, Munich, Germany, 5–9 October 2015*; Proceedings, Part III 18; Springer International Publishing: Berlin/Heidelberg, Germany, 2015; pp. 234–241.

19. Gu, Z.; Chai, X.; Yang, T. Deep-Learning-Based Low-Frequency Reconstruction in Full-Waveform Inversion. *Remote Sens.* **2023**, *15*, 1387. [CrossRef]
20. Parasyris, A.; Stankovic, L.; Stankovic, V. Synthetic Data Generation for Deep Learning-Based Inversion for Velocity Model Building. *Remote Sens.* **2023**, *15*, 2901. [CrossRef]
21. Zhang, H.; Zhu, P.; Liao, Z. SaltISNet3D: Interactive Salt Segmentation from 3D Seismic Images Using Deep Learning. *Remote Sens.* **2023**, *15*, 2319. [CrossRef]
22. Tao, L.; Ren, H.; Gu, Z. Acoustic Impedance Inversion from Seismic Imaging Profiles Using Self Attention U-Net. *Remote Sens.* **2023**, *15*, 891. [CrossRef]
23. Xiong, P.; Marchetti, D.; De Santis, A.; Zhang, X.; Shen, X. SafeNet: SwArm for Earthquake Perturbations Identification Using Deep Learning Networks. *Remote Sens.* **2021**, *13*, 5033. [CrossRef]
24. Sun, H.; Demanet, L. Deep Learning for Low-Frequency Extrapolation of Multicomponent Data in Elastic FWI. *IEEE Trans. Geosci. Remote Sens.* **2022**, *60*, 5909511. [CrossRef]
25. Wang, S.; Han, L.; Gong, X.; Zhang, S.; Huang, X.; Zhang, P. MCMC Method of Inverse Problems Using a Neural Network—Application in GPR Crosshole Full Waveform Inversion: A Numerical Simulation Study. *Remote Sens.* **2022**, *14*, 1320. [CrossRef]
26. Liu, N.; Chen, J.; Wu, H.; Li, F.; Gao, J. Microseismic First-Arrival Picking Using Fine-Tuning Feature Pyramid Networks. *IEEE Geosci. Remote Sens. Lett.* **2022**, *19*, 7505105. [CrossRef]
27. Lou, Y.; Li, S.; Li, S.; Liu, N.; Zhang, B. Seismic Volumetric Dip Estimation via Multichannel Deep Learning Model. *IEEE Trans. Geosci. Remote Sens.* **2022**, *60*, 4511014. [CrossRef]
28. Dou, Y.; Li, K.; Duan, H.; Li, T.; Dong, L.; Huang, Z. MDA GAN: Adversarial-Learning-Based 3-D Seismic Data Interpolation and Reconstruction for Complex Missing. *IEEE Trans. Geosci. Remote Sens.* **2023**, *61*, 5905014. [CrossRef]
29. Roux, P.; Sabra, K.G.; Gerstoft, P.; Kuperman, W.A.; Fehler, M.C. P-waves from cross-correlation of seismic noise. *Geophys. Res. Lett.* **2005**, *32*. [CrossRef]
30. Snieder, R.; Sheiman, J.; Calvert, R. Equivalence of the virtual-source method and wave-field deconvolution in seismic interferometry. *Phys. Rev. E* **2006**, *73*, 066620. [CrossRef] [PubMed]
31. Nakata, N.; Snieder, R.; Tsuji, T.; Larner, K.; Matsuoka, T. Shear wave imaging from traffic noise using seismic interferometry by cross-coherence. *Geophysics* **2011**, *76*, SA97–SA106. [CrossRef]
32. Wapenaar, K.; Van Der Neut, J.; Ruigrok, E.; Draganov, D.; Hunziker, J.; Slob, E.; Thorbecke, J.; Snieder, R. Seismic interferometry by crosscorrelation and by multidimensional deconvolution: A systematic comparison. *Geophys. J. Int.* **2011**, *185*, 1335–1364. [CrossRef]
33. Oktay, O.; Schlemper, J.; Folgoc, L.L.; Lee, M.; Heinrich, M.; Misawa, K.; Mori, K.; McDonagh, S.; Hammerla, N.Y.; Kainz, B.; et al. Attention u-net: Learning where to look for the pancreas. *arXiv* **2018**, arXiv:1804.03999.
34. Woo, S.; Park, J.; Lee, J.Y.; Kweon, I.S. CBAM: Convolutional Block Attention Module. In Proceedings of the European Conference on Computer Vision (ECCV), Munich, Germany, 8–14 September 2018.
35. Wapenaar, K.; van der Neut, J.; Ruigrok, E. Passive seismic interferometry by multidimensional deconvolution. *Geophysics* **2008**, *73*, A51–A56. [CrossRef]
36. Sun, H.; Demanet, L. Beyond Correlations: Deep Learning for Seismic Interferometry. *IEEE Trans. Neural Netw. Learn. Syst.* **2023**, *34*, 3385–3396. [CrossRef]